

Nanoindentation of binary and ternary Ni–Ti-based shape memory alloy thin films

A.J. Muir Wood^a, S. Sanjabi^b, Y.Q. Fu^c, Z.H. Barber^a, T.W. Clyne^{a,*}

^a Department of Materials Science & Metallurgy, Cambridge University, Pembroke Street, Cambridge CB2 3QZ, UK

^b Department of Materials Science and Engineering, Faculty of Engineering, Tarbiat Modares University PO Box 14115-143, Tehran, Iran

^c Department of Mechanical Engineering, Heriot-Watt University, Edinburgh, EH14 4AS, UK

Received 27 August 2007; accepted in revised form 12 November 2007

Available online 21 November 2007

Abstract

Thin sputtered films of binary (Ni–Ti) and ternary (Ni–Ti–Hf and Ni–Ti–Cu) shape memory alloys have been subjected to nanoindentation over a range of temperature (up to 400 °C), using a small diameter spherical indenter. The load-displacement plots obtained during these experiments have been interpreted so as to reveal whether the imposed strain was being at least partly accommodated by the martensitic phase transformation, ie whether superelastic deformation was taking place. This was done by evaluating the remnant indent depth ratio (depth after unloading/depth at peak load), which is expected to have a relatively small value if superelastic deformation and recovery are significant. It is confirmed that this procedure, which has previously been validated for bulk material, can be applied to these thin films (~2 μm in thickness). The results indicate that ternary alloys with up to about 20 at.%Hf or 10 at.%Cu can exhibit superelastic behaviour over suitable temperature ranges. © 2007 Elsevier B.V. All rights reserved.

Keywords: Nickel–titanium; Nickel–titanium–copper; Nickel–titanium–hafnium; Thin film; Shape memory; Indentation

1. Introduction

Thin films of shape memory alloys (SMAs) are of growing interest, particularly for various small scale devices. Thin films of Ni–Ti binary alloys have been extensively studied [1–17] and the effects of alloying additions, particularly copper and hafnium, on the transformation characteristics have also been subjected to close scrutiny [18–27]. The addition of Hf stabilises the shape memory effect (SME) and superelasticity (SE) to higher temperatures, generating what are sometimes known [25–32] as high temperature shape memory alloys (HTSMAs). These have been quite widely investigated, but the difficulty and cost of alloying bulk Ni–Ti with such ternary additions has proved problematic. Compositional control in these systems is easier with thin films, giving a further incentive for their study. The addition of Cu to Ni–Ti is also of interest. This does not increase the transformation temperatures, but it can raise the stability of the alloy during temperature changes and mechan-

ical loading. The mechanism for this effect is thought [33] to involve inhibiting the nucleation and growth of both R-phase and Ni₄Ti₃ precipitates. The addition of Cu also reduces hysteresis effects during thermal cycling. Copper is soluble in NiTi at levels of up to ~20 at.%, replacing the Ni on the lattice sites [34]. Above this level, other phases form, limiting the SME. However, the effective upper limit for Cu additions is actually ~10 at.%, above which it causes severe embrittlement [33,35].

A number of studies have previously been carried out involving nanoindentation of shape memory alloys, in both bulk [36–38] and thin film [3,9,39–42] forms. However, only recently has it been clearly shown [43] that, by focussing on the remnant depth ratio and testing over a range of temperature, indentation load-displacement data can be interpreted to reveal whether a (bulk) material is exhibiting SE (deforming primarily via strain-induced phase transformations). A remnant depth ratio that shows evidence of superelasticity is not revealed using a Berkovich tip, since the strains beneath a Berkovich tip exceed the superelastic limit and the resulting deformation is plastic. Using a spherical tip, where strains can be minimised, deformation can be kept below the superelastic limit and

* Corresponding author.

E-mail address: twc10@cam.ac.uk (T.W. Clyne).

Table 1
Compositions and measured transformation temperatures for the thin films studied

Code	Composition	A_s	A_f	R_s	R_f	M_s	M_f
TF1	Ni _{47.2} Ti _{52.8}	60 °C	70 °C	70 °C	40 °C	40 °C	35 °C
TF2	Ni _{49.4} Ti _{50.6}	75 °C	85 °C	50 °C	40 °C	40 °C	20 °C
TF3	Ni _{51.2} Ti _{48.8}	10 °C	20 °C	40 °C	30 °C	-40 °C	-50 °C
TF4	Ni _{49.6} Ti _{45.2} Hf _{5.2}	-25 °C	35 °C	25 °C	10 °C	-45 °C	-55 °C
TF5	Ni _{49.4} Ti _{40.2} Hf _{10.4}	85 °C	110 °C	100 °C	70 °C	70 °C	50 °C
TF6	Ni _{49.5} Ti _{34.9} Hf _{15.6}	150 °C	160 °C	125 °C	100 °C	100 °C	80 °C
TF7	Ni _{49.2} Ti _{29.7} Hf _{21.1}	220 °C	250 °C	–	–	200 °C	170 °C
TF8	Ni _{49.3} Ti _{26.3} Hf _{24.4}	385 °C	415 °C	–	–	360 °C	330 °C
TF9	Ni _{49.2} Ti _{22.1} Hf _{28.7}	>400 °C	>400 °C	–	–	>400 °C	>400 °C
TF10	Ni _{47.6} Ti ₅₁ Cu _{1.4}	70 °C	75 °C	–	–	50 °C	40 °C
TF11	Ni _{40.2} Ti ₅₁ Cu _{8.8}	45 °C	55 °C	–	–	40 °C	30 °C
TF12	Ni _{34.4} Ti ₅₃ Cu _{12.6}	50 °C	60 °C	–	–	50 °C	40 °C

superelasticity can be studied. Moreover, no studies of this type have previously been applied to thin films or to Ni–Ti alloys with ternary additions. In the present work, these procedures are applied to thin Ni–Ti–X films with a range of compositions.

2. Experimental procedures

Thin films, either binary alloys of Ni–Ti or ternary alloys of Ni–Ti with Cu or Hf additions, were produced by ultra high vacuum DC magnetron sputtering onto unheated Si (100) substrates with dimensions of 10 × 5 mm. Deposition was under a constant flow of Ar (99.999%) and the substrate was rotated at 10 rpm during deposition. More details concerning preparation of these films, and some characterisation work, are described elsewhere [16,27,44–46]. The films were typically about 2 μm in thickness. The alloys studied, and the code numbers of these specimens, are shown in Table 1. Film compositions were verified by energy dispersive X-ray analysis, using a JEOL 5800 LV scanning electron microscope (SEM). Transformation temperatures were determined by differential scanning calorimetry (DSC), using a Q1000 Thermal Analysis instrument.

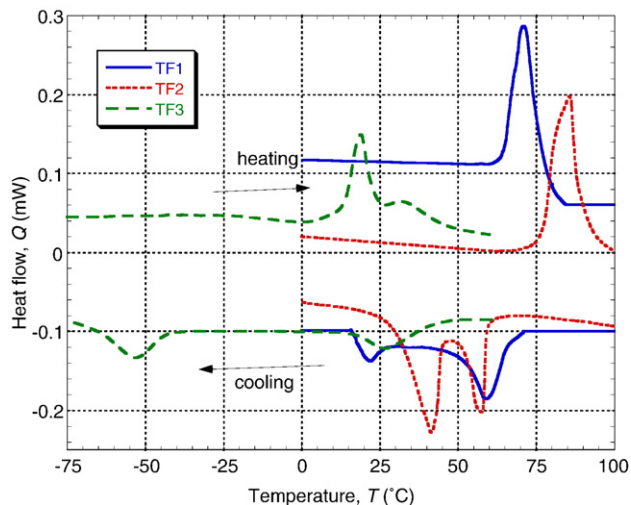


Fig. 1. DSC data for binary Ni–Ti thin films. (See Table 1 for film compositions).

Both room temperature and high temperature X-ray diffraction (XRD) were performed, using a Siemens D500 X-ray diffractometer with a $\text{CuK}\alpha$ ($\lambda=1.54056 \text{ \AA}$) X-ray source. All indentation experiments were performed using a MicroMaterials machine, employing the NanoTest pendulum. Indentation was undertaken using a spherical tip ($r=10 \text{ }\mu\text{m}$), fitted with a heater to allow high temperature indentation, in conjunction with a sample heating stage. Indentation was to depths of up to 10% of the film thickness which was generally 200 nm, with an indentation rate of $\sim 3\text{--}5 \text{ nm s}^{-1}$. Experiments were conducted (in air) at up to 400 °C. Neither tip nor specimen exhibited any significant oxidation or other degradation during these operations.

3. Results and discussion

3.1. Phase transformations and hysteresis behaviour

DSC results for the binary alloy thin films, TF1 (Ti-rich), TF2 (approximately equiatomic) and TF3 (Ni-rich), are shown

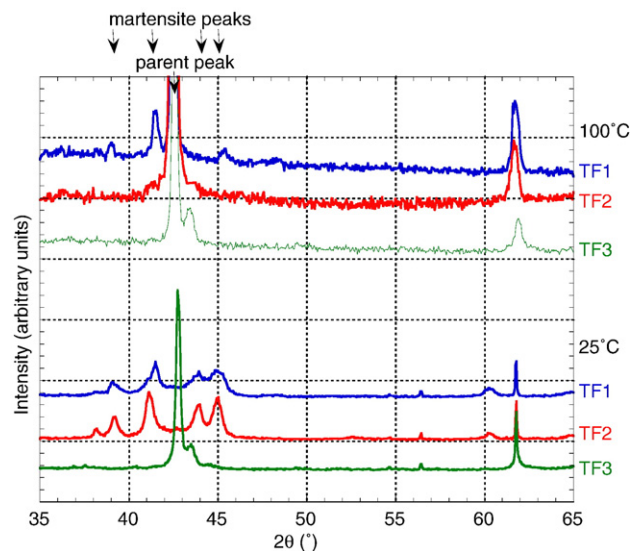


Fig. 2. XRD spectra for binary Ni–Ti thin films, obtained at two different temperatures.

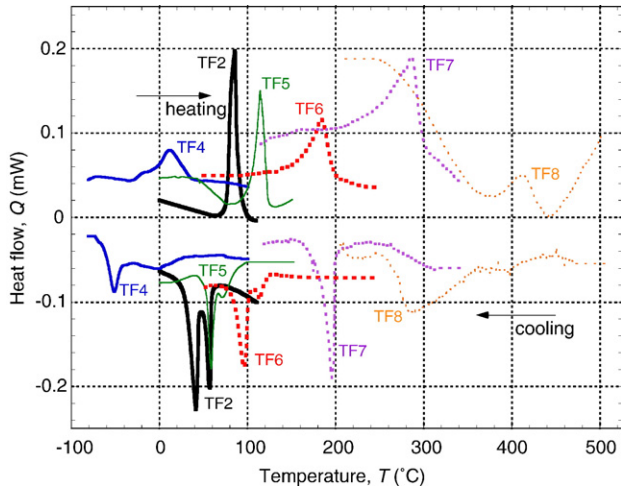


Fig. 3. DSC data for ternary Ni–Ti–Hf thin films. (See Table 1 for film compositions).

in Fig. 1. These clearly demonstrate that all three films undergo shape memory transformations in the range $-100\text{ }^{\circ}\text{C}$ to $100\text{ }^{\circ}\text{C}$. Furthermore, it can be seen that, while TF1 and TF2 are primarily martensitic at room temperature, the Ni-rich (TF3) specimen is in the parent phase at this temperature. XRD data (Fig. 2) confirm this, and also indicate that, on heating to $100\text{ }^{\circ}\text{C}$, all three films become primarily parent phase. Superelastic behaviour would thus be expected from all three films at around $100\text{ }^{\circ}\text{C}$. The compositions and transformation temperatures of these three films are listed in Table 1.

Similar results were obtained for the Ni–Ti–Hf thin films, as shown in Figs. 3 and 4. The DSC plots in Fig. 3 confirm that transformation temperatures can be raised by Hf additions. However, it can be seen that a small addition of Hf (5.2 at.%), specimen TF4, actually reduces the transformation tempera-

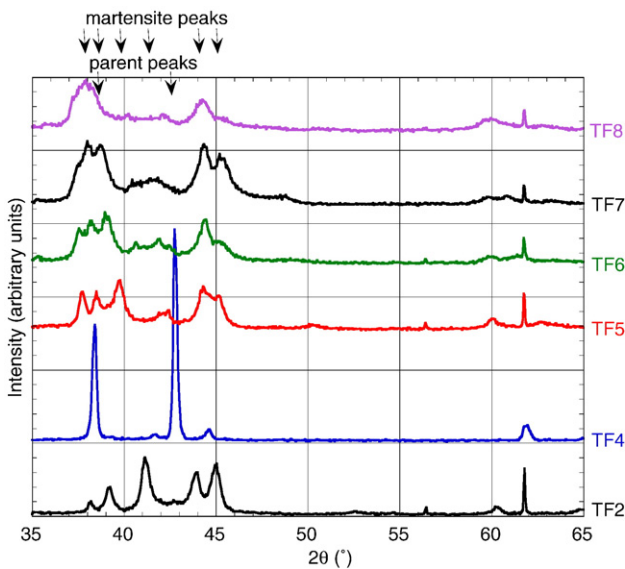


Fig. 4. XRD data for ternary Ni–Ti–Hf thin films, obtained at room temperature.

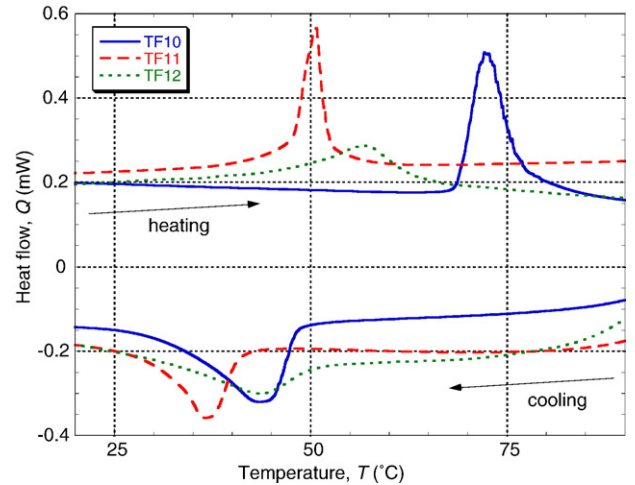


Fig. 5. DSC data for ternary Ni–Ti–Cu thin films. (See Table 1 for film compositions).

res, when compared with the equivalent binary Ni–Ti film. This is consistent with previous observations. It is not until the Hf level reaches 10.4 at.% (specimen TF5) that the transformation temperatures exceed those of the equivalent binary alloy. The magnitude of the transformation peaks diminishes with increasing Hf content. This is expected, since the volume of transformable material is known [18] to decrease as the Hf content is raised. Specimen TF9, containing 28.7 at.% Hf, did not exhibit any detectable transformation peaks. The XRD data (Fig. 4) show that, while specimen TF4 (5.2 at.% Hf) is in the parent phase at that temperature, all other Hf-containing films are in the martensitic phase at that temperature, and will thus require heating in order for any SE to be observed. The peak broadening observed in films with high Hf contents is presumably caused by the introduction of defects, with the Ni–Ti lattice structure becoming distorted as substitution of Ti by (larger)

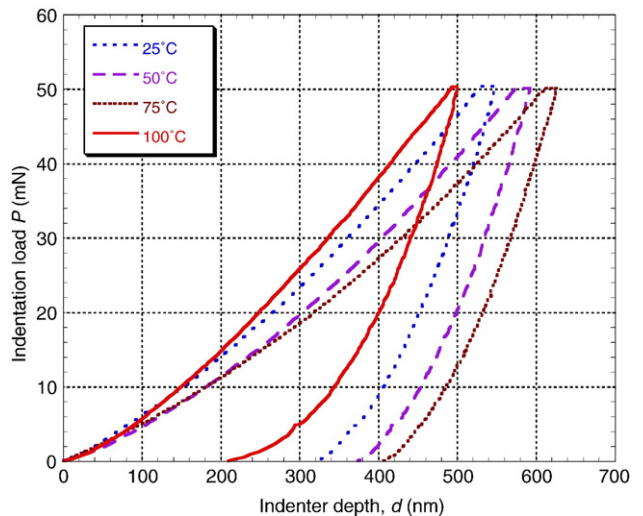


Fig. 6. Load-displacement plots obtained during indentation carried out at various temperatures around and below A_B using a small spherical ($r=10\text{ }\mu\text{m}$) indenter. The dwell period at maximum load was 10 s.

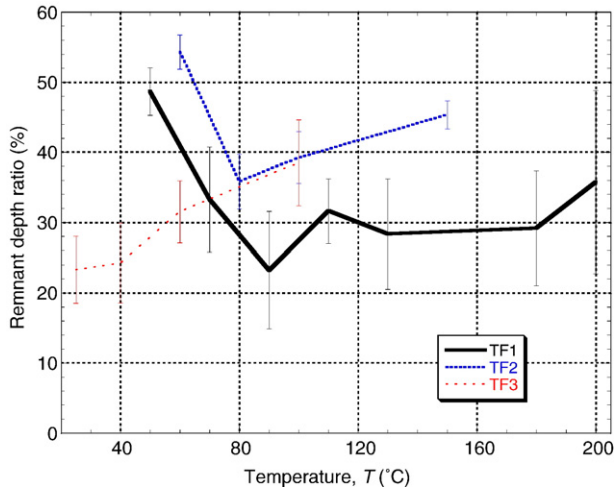


Fig. 7. Plots of remnant depth ratio as a function of test temperature, for the three different binary Ni–Ti alloys. The maximum indentation depth was 200 nm in all cases. Corresponding A_f temperatures are about 70 °C, 85 °C and 20 °C respectively for specimens TF1, TF2 and TF3.

Hf atoms takes place. A reduction in Ni–Ti–Hf crystallite size, as a consequence of a limitation on the concentration of (Ti, Hf)₂Ni precipitates [28,47], may also be contributing to this effect.

The DSC data for the Ni–Ti–Cu thin films (Fig. 5) show that all three compositions would be expected to exhibit shape memory transformations between room temperature and 100 °C. As discussed above, unlike Hf substitution for Ti, Cu substitution for Ni does not increase the transformation temperatures, but rather stabilises the alloy and reduces the hysteresis. In fact, the values of A_s and M_s are approximately coincident (at about 50 °C) for TF12 (12.5 at.%Cu). The transformation temperatures and compositions of these films are listed in Table 1.

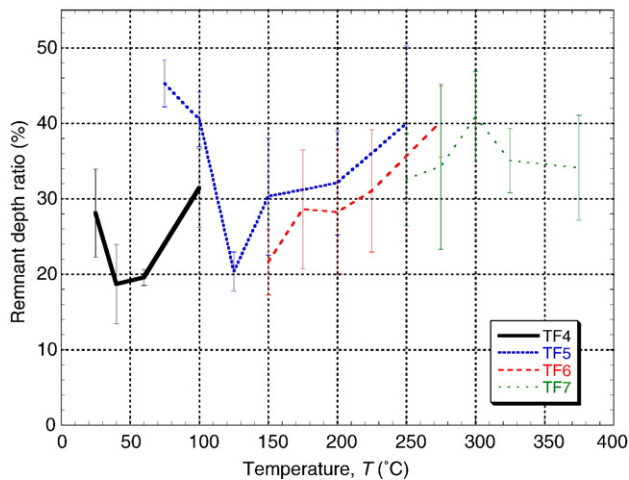


Fig. 8. Plots of remnant depth ratio as a function of test temperature, for ternary Ni–Ti–Hf alloys. The maximum indentation depth was 200 nm in all cases. Corresponding A_f temperatures are about 35 °C, 110 °C, 160 °C and 250 °C respectively for specimens TF4, TF5, TF6 and TF7.

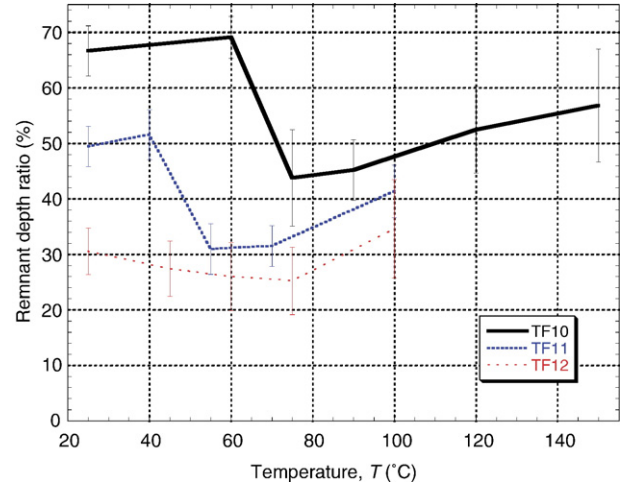


Fig. 9. Plots of remnant depth ratio as a function of test temperature, for ternary Ni–Ti–Cu alloys. The maximum indentation depth was 200 nm in all cases. Corresponding A_f temperatures are about 75 °C, 55 °C and 60 °C respectively for specimens TF10, TF11 and TF12.

3.2. Indentation

As mentioned above, it was shown in previous work [43] that SE can be detected experimentally in bulk shape memory

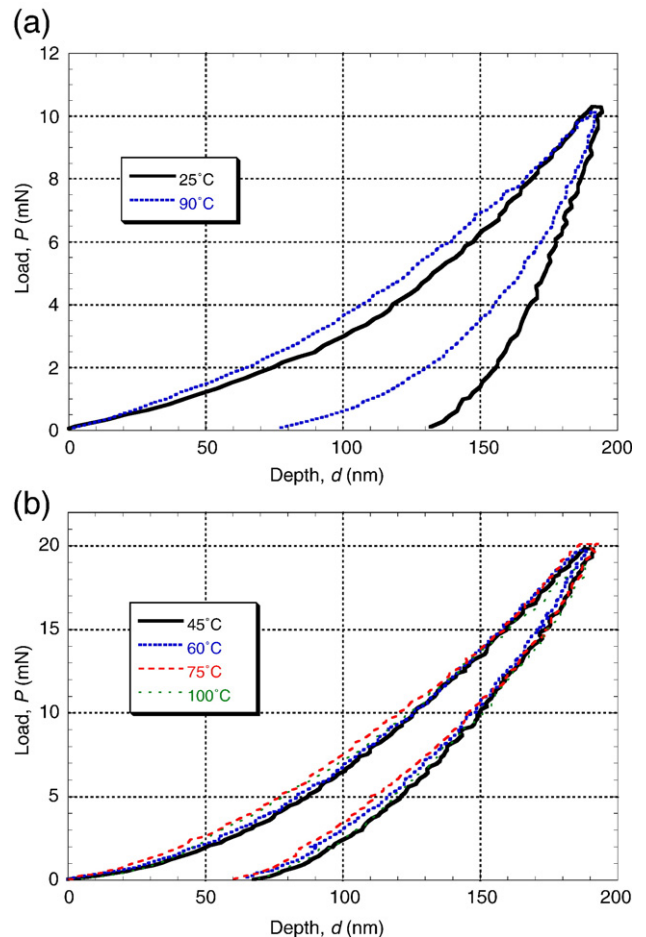


Fig. 10. Indentation load-displacement plots above and below A_f for (a) specimen TF10 ($A_f = 75$ °C) and (b) specimen TF12 ($A_f = 60$ °C).

materials. This is most effectively done by using a spherical indenter and focussing on the dependence of the measured remnant depth ratio on temperature, across the range over which the contribution of SE to the total plastic strain is expected to change from substantial to negligible. This is illustrated by Fig. 6, which shows the change in indentation response with temperature for a binary shape memory alloy (Ti — 50.2 at.%Ni), with $A_f \sim 100$ °C. As the temperature is increased (below A_f), the indentation depth gradually increases, as would be expected. Above A_f , the indentation depth drops to below the level seen at room temperature, as expected given the phase transformation. The remnant depth ratio, however, also drops dramatically (ie the indent recovers much more significantly above 100 °C), demonstrating the superelastic recovery of the indent. Plots of remnant depth ratio against temperature thus give a good indication of whether superelasticity is taking place.

In the present work, indentation experiments were conducted first on the binary thin films, in order to verify that it was indeed possible to observe SE in thin film samples, despite the low depths and loads required. The measured variation in remnant depth ratio with temperature for these three films is shown in Fig. 7. As was observed for bulk materials [43], a drop in remnant depth ratio is seen on increasing the temperature above A_f . This regime of low remnant depth ratio reflects conditions favourable for SE to occur (an initial structure which is predominantly parent phase and the stress required for this phase to deform by conventional dislocation motion being higher than that needed to induce formation of the martensitic phase). Specimen TF3, which was in the parent phase at room temperature, shows a decay of SE with increasing temperature from the start, manifest as an increase in remnant depth ratio, as competing modes of plastic deformation (notably dislocation motion) become energetically more favourable than the (reversible) SE transformation to the martensitic phase. This also occurs with the other two films, but the onset of SE is delayed in those cases until the temperature is sufficiently high to ensure that the starting material is predominantly in the parent phase.

Indentation of the Ni–Ti–Hf ternary films showed clear evidence of this transition to SE deformation as the starting material became predominantly parent phase (Fig. 8), at least for those samples containing less than 20 at.%Hf. Specimen TF4, which was in the parent phase at room temperature, and specimens TF5 and TF6, all demonstrate an increase in remnant depth ratio as the temperature is increased above A_f and dislocation mechanisms start to dominate. For specimen TF7 (21.1 at.%Hf), however, the behaviour is slightly different, with less change in remnant depth ratio on heating through A_f . It may be that the SE effect cannot operate effectively at these relatively high temperatures. In any event, the DSC and XRD data suggest that high Hf contents reduce the volume of material capable of exhibiting SE. This is consistent with previous work [18] and the high content of precipitates reported at high Hf levels is certainly expected to inhibit SE transformations.

Similar behaviour was observed for the Ni–Ti–Cu ternary films (Fig. 9). While evidence of SE deformation is observed above A_f for specimens TF10 (1.4 at.%Cu) and TF11

(8.8 at.%Cu), no evidence of SE is seen for specimen TF12 (12.6 at.%Cu). Copper is soluble in Ni–Ti up to 20 at.% but the material becomes very brittle [33,35] above 10 at.%. It therefore seems likely that, while SE might have been expected in TF12 above A_f (60 °C), permanent deformation mechanisms (probably including microcracking) are likely to dominate throughout. Study of the individual load-displacement plots for TF10 and TF12 provides evidence for this — see Fig. 10. While the difference between the responses of the parent and martensitic phases is obvious for TF10 (Fig. 10)(a), there is no noticeable difference in the response of TF12 as it is heated through and above A_f (Fig. 10)(b).

4. Conclusions

The following conclusions can be drawn from this work.

- (a) Thin films of binary Ni–Ti alloys and ternary Ni–Ti–Hf and Ni–Ti–Cu alloys have been studied in terms of their phase transformation characteristics and subjected to indentation over a range of temperature. The remnant depth ratio (unloaded indent depth/maximum indent depth) can be used as a parameter to explore whether the plastic strain imposed by the indentation is being primarily accommodated by superelastic deformation (parent-martensite phase transformation). A low ratio (substantial recovery) suggests that superelasticity is occurring. A spherical indenter has been used, which generates relatively low peak strains in the indented material, and hence favours superelasticity, which is unable to accommodate large strains.
- (b) Indentation of the binary alloy films confirmed that this technique can reliably reveal whether superelasticity is occurring during particular indentation experiments, with films of this thickness (~ 2 μm). Typically, a noticeable drop in remnant depth ratio is observed as the testing temperature is raised sufficiently to ensure that the starting material is predominantly in the parent phase.
- (c) Indentation of the ternary alloy films containing Hf confirmed that they can exhibit superelasticity with up to ~ 20 at.%Hf. Above this level, it appears that little or no superelastic deformation occurs, probably because the microstructure contains a high volume fraction of non-transformable precipitates.
- (d) Indentation of the ternary alloy films containing Cu showed that superelastic behaviour is possible with up to about 10 at.%Cu. Above this level, superelasticity seems to be inhibited. It is suggested that this is attributable to the brittleness known to be introduced by such high Cu levels, leading to high levels of fine scale microcracking, or other defect generation, and thus inhibiting superelastic deformation and recovery during indentation.

Acknowledgements

Support for AJMW has been provided via an EPSRC studentship, while SS has been supported via the British Council in Tehran.

References

- [1] J.D. Busch, A.D. Johnson, C.H. Lee, D.A. Stevenson, *J. Appl. Phys.* 68 (1990) 6224.
- [2] S. Miyazaki, A. Ishida, *Mater. Sci. Eng., A Struct. Mater.: Prop. Microstruct. Process.* 273–275 (1999) 106.
- [3] S. Moyne, C. Poilane, K. Kitamura, S. Miyazaki, P. Delobelle, C. LExcellent, *Mater. Sci. Eng., A Struct. Mater.: Prop. Microstruct. Process.* 273–275 (1999) 727.
- [4] P. Chen, J.M. Ting, *Thin Solid Films* 398–399 (2001) 597.
- [5] Y. Fu, W. Huang, H. Du, X. Huang, J. Tan, X. Gao, *Surf. Coat. Technol.* 145 (2001) 107.
- [6] J.X. Zhang, M. Sato, A. Ishida, *Acta Mater.* 49 (2001) 3001.
- [7] F.M.B. Fernandes, R. Martins, M.T. Nogueira, R.J.C. Silva, P. Nunes, D. Costa, I. Ferreira, R. Martins, *Sens. Actuators A: Phys.* 99 (2002) 55.
- [8] C. Craciunescu, J. Li, M. Wuttig, *Scr. Mater.* 48 (2003) 65.
- [9] G.A. Shaw, D.S. Stone, A.D. Johnson, A.B. Ellis, W.C. Crone, *Appl. Phys. Lett.* 83 (2003) 257.
- [10] Y. Fu, H. Du, W. Huang, S. Zhang, M. Hu, *Sens. Actuators A: Phys.* 112 (2004) 395.
- [11] Q. He, W.M. Huang, M.H. Hong, M.J. Wu, Y.Q. Fu, T.C. Chong, F. Chellet, H.J. Du, *Smart Mater. Struct.* 13 (2004) 977.
- [12] B.K. Lai, H. Kahn, S.M. Phillips, Z. Akase, A.H. Heuer, *J. Mater. Res.* 19 (2004) 2822.
- [13] J.X. Zhang, M. Sato, A. Ishida, *Smart Mater. Struct.* 13 (2004) N37.
- [14] M.A. Arranz, J.M. Riveiro, J. Magn. Magn. Mater. 290–291 (2005) 865.
- [15] H. Ni, H.J. Lee, A.G. Ramirez, *J. Mater. Res.* 20 (2005) 1728.
- [16] S. Sanjabi, S.K. Sadrnezhad, K.A. Yates, Z.H. Barber, *Thin Solid Films* 491 (2005) 190.
- [17] Z.Y. Yuan, D. Xu, Z.C. Ye, B.C. Cai, *Mater. Sci. Technol.* 21 (2005) 319.
- [18] D.R. Angst, P.E. Thoma, M.Y. Kao, *J. Phys. IV C8* (1995) 747.
- [19] X.L. Meng, Y.F. Zheng, Z. Wang, L.C. Zhao, *Mater. Lett.* 45 (2000) 128.
- [20] X.L. Meng, W. Cai, L.M. Wang, Y.F. Zheng, L.C. Zhao, L.M. Zhou, *Scr. Mater.* 45 (2001) 1177.
- [21] J. Uchil, K.K. Mahesh, K. Ganesh Kumara, *J. Mater. Sci.* 36 (2001) 5823.
- [22] M. Hosogi, T. Sakuma, N. Okabe, K. Okita, *Mater. Sci. Forum* 394–395 (2002) 253.
- [23] X.L. Meng, W. Cai, Y.F. Zheng, Y.X. Tong, L.C. Zhao, L.M. Zhou, *Mater. Lett.* 55 (2002) 111.
- [24] H. Scherngell, A.C. Kneissl, *Acta Mater.* 50 (2002) 327.
- [25] X. Meng, W. Cai, K.T. Lau, L.M. Zhou, L. Zhao, *Mat. Sci. & Tech.* 19 (2003) 590.
- [26] G.S. Firstov, J. Van Humbeeck, Y.N. Koval, *Mater. Sci. Eng., A Struct. Mater.: Prop. Microstruct. Process.* 378 (2004) 2.
- [27] S. Sanjabi, Y.Z. Cao, Z.H. Barber, *Sens. Actuators A: Phys.* 121 (2005) 543.
- [28] X.D. Han, W.H. Zou, R. Wang, Z. Zhang, D.Z. Yang, K.H. Wu, *J. Phys. IV C8* (1995) 753.
- [29] J. Van Humbeeck, *J. Eng. Mater. Technol.–Trans. ASME* 121 (1999) 98.
- [30] X.L. Meng, W. Cai, Y.F. Zheng, Y.B. Rao, L.C. Zhao, *Mater. Lett.* 57 (2003) 4206.
- [31] X.L. Meng, Y.F. Zheng, W. Cai, L.C. Zhao, *J. Alloys Compd.* 372 (2004) 180.
- [32] X.L. Meng, Y. Wu, W. Cai, L.C. Zhao, *Trans. Nonferrous Metals Soc. China* 15 (2005) 340.
- [33] T. Saburi, in: K. Otsuka, CM Wayman (Eds.), *Ti–Ni Shape Memory Alloys*, in *Shape Memory Materials*, CUP, Cambridge, 1998, p. 49.
- [34] K.P. Gupta, *J. Phase Equilibria* 23 (2002) 541.
- [35] J. Van Humbeeck, R. Stalmans, in: M. Schwartz (Ed.), *Encyclopaedia of Smart Materials*, John Wiley and Sons, Inc., 2002, p. 951.
- [36] H. Pelletier, D. Muller, P. Mille, J.J. Grob, *Surf. Coat. Technol.* 158–159 (2002) 309.
- [37] W. Ni, Y.T. Cheng, D.S. Grummon, *Appl. Phys. Lett.* 80 (2002) 3310.
- [38] K. Gall, K. Juntunen, H.J. Maier, H. Sehitoglu, Y.I. Chumlyakov, *Acta Mater.* 49 (2001) 3205.
- [39] H.D. Espinosa, B.C. Prorok, M. Fischer, *J. Mech. Phys. Solids* 51 (2003) 47.
- [40] W. Ni, Y.T. Cheng, M. Lukitsch, A.M. Weiner, L.C. Lev, D.S. Grummon, *Wear* 259 (2005) 842.
- [41] X.G. Ma, K. Komvopoulos, *Appl. Phys. Lett.* 83 (2003) 3773.
- [42] X.G. Ma, K. Komvopoulos, *Appl. Phys. Lett.* 84 (2004) 4274.
- [43] A.J. Muir Wood, T.W. Clyne, *Acta Mater.* 54 (2006) 5607.
- [44] H.J. Du, Y.Q. Fu, *Surf. Coat. Technol.* 176 (2004) 182.
- [45] S. Sanjabi, Y.Z. Cao, S.K. Sadrnezhad, Z.H. Barber, *J. Vac. Sci. Technol., A, Vac. Surf. Films* 23 (2005) 1425.
- [46] Y.Q. Fu, H.J. Du, S. Zhang, Y.W. Gu, *Surf. Coat. Technol.* 198 (2005) 398.
- [47] P. Olier, J.C. Brachet, J.L. Bechade, C. Foucher, G. Guénin, *J. Phys. IV C8* (1995) 741.